<div align="center">

ELECTRONIC SUPPLEMENTARY INFORMATION FOR PUBLICATION
Critical STEP Advances for Sustainable Iron Production

</div>

*Baochen Cui[a] and Stuart Licht,[*a]*
[a]Department of Chemistry, George Washington University, Washington, DC 20052, USA.
CORRESPONDING AUTHOR EMAIL ADDRESS: slicht@gwu.edu

Expanded introduction, methodology details, and electrochemical parameter optimization

Along with control of fire and the production of cement, the carbothermal reduction of iron is one of the founding technological pillars of civilization. Yet, it is also one of the major global sources of greenhouse gas release, and a CO_2–free process to form this staple is needed. Hematite, Fe_2O_3, and magnetite, Fe_3O_4, are the principal ores currently used for the widespread carbothermal industrial production of iron. Introduced in 2010, STEP Iron produces iron without carbon dioxide emission through a new chemistry consisting of the electrochemical reduction of the unexpected, high solubility of Fe_2O_3 and Fe_3O_4 in molten lithiated carbonates.[1] This electronic supplementary information systematically characterizes the critical electrochemistry of STEP Iron, to provide high coulombic efficiency (approaching a 100% yield of the 3 e- reduction of Fe_2O_3), low electrolysis potential and kinetically facile electron transfer to provide high rate. The electronic supplementary information provides a consistent analytical methodology to access iron purity, as well as specific, useful cathode, anode and electrolyte configurations to sustainably and effectively produce iron without greenhouse gas emissions.

The electrolytic formation of energetic materials dates back to the first splitting of water to hydrogen and oxygen in 1801 and the discovery of the element potassium by Lavosier in 1807. By the 1900's the decrease in standard electrochemical potential (unit activity) with increasing temperature of a variety of half reactions was well established,[ESI-1] and by the 1980's investigators such as Bockris[ESI-2] suggested the use of thermal energy, including via nuclear or solar energy, to decrease the electrolysis potential required to drive water splitting. Solar splitting at elevated temperatures combines elements of solid state physics, insolation (solar radiation reaching a given area) and electrochemical theory, complicating any rigorous theoretical support of the process. In 2002, we derived the first rigorous theory that a solar photon contains sufficient thermal and electronic energy to efficiently split water by electrolysis.[ESI-3] This led in 2003 to the first experimental demonstration that a single semiconductor with a bandgap of less than the electrochemical potential to split water ($E°_{H_2O}(25°C) = 1.23V$), such as silicon ($E_{bandgap} = 1.1$ V), can directly drive solar water splitting (in molten hydroxide) by applying the excess solar thermal energy (not used by the silicon).[ESI-4] The 2002 theory and experiment was generalized, from water splitting and hydrogen fuel formation, to all endothermic electrochemical processes in 2009 with the acronym STEP.[1]

STEP and conventional iron chemistries. Commercial iron today continues to be produced by the millennia old carbothermal process. In the carbothermal process iron oxide is reduced by carbon. The carbothermal process releases the greenhouse gas, CO_2, for example in the 3 electron reduction of Fe(III), accompanied by the 4 electron oxidation of carbon, as illustrated on the left side of Figure 1.

$$2Fe_2O_3 + 3C \rightarrow 4Fe + 3CO_2 \qquad \Delta H_{298} = 466.4 \text{ kJ/mol} \qquad (1)$$

This Fe_2O_3 reduction reaction is endothermic. To sustain this reaction, heat, ΔH, is provided by the burning of over one additional carbon, with concurrent release of further carbon dioxide:

$$C + O_2 \rightarrow CO_2 \qquad \Delta H_{298} = -393.5 \text{ kJ/mol} \qquad (2)$$

Alternatively, iron oxide can be electrolyzed, producing iron metal and evolving only oxygen, without carbon dioxide release. For example via:

$$Fe_2O_3 \rightarrow 2Fe + 3/2O_2; \qquad E°(25°, 750°C \text{ or } 1000°C) = 1.28 \text{ V}, \ 0.96 \text{ V, or } 0.85 \text{ V} \qquad (3)$$
$$Fe_3O_4 \rightarrow 3Fe + 2O_2; \qquad E°(25°, 750°C \text{ or } 1000°C) = 1.32 \text{ V or } 1.01V, \ 0.92 \text{ V} \qquad (4)$$
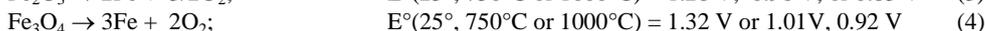
STEP and conventional carbon footprint. *No CO_2 is released in this STEP process* when the heat and electronic charge is generated by renewable energy (solar, wind, hydro, geothermal) or nuclear energy. Alternatively, we can calculate the CO_2 release when fossil fuels are used to form the electricity. As demonstrated in this study, iron may be formed at an electrolysis potential of as little as 0.9V in molten as Li_2CO_3. In Equation iii, the room temperature rest potential (calculated from the free energy of the reaction) is 1.28 V and the thermoneutral potential (calculated from the enthalpy of the reaction) is 1.43 V. The latter voltage is the energy required to prevent the system from cooling during electrolysis, and unlike the endothermic rest potential, is nearly constant with changing temperature, for example, $E_{thermoneutral}(1200°C) = 1.40$ V, and from Equation iii requires 6 Faraday per mole of iron. This is equivalent to 0.225 kWh / mol Fe (from F = 96,485 A sec, and 1 kW=1000 VA), and will be less if an alternate heat source is used to maintain the system electrolysis temperature. Currently, fossil fuels release ~11 mol CO_2 / kWh; specifically the natural gas, oil, and coal generation of electricity have respective stack emissions of 7.5, 12 and 15 mol CO_2 / kWh. Hence, even if fossil fuel, rather than renewable energy, is used to generate the heat and electricity and heat for iron by electrolysis, it will only emit 0.225 x 11 = 2.5 CO_2 per Fe generated. This is less than the 7 CO_2 per Fe emitted by the existing iron smelting processes. In summary:

Iron generation Process	CO_2 emitted per Fe generated
conventional smelting	7
new Li_2CO_3 electrolysis powered by fossil fuel electricity	2.5
STEP Li_2CO_3 (solar) electrolysis	0

Eqs. 2 and 3 endothermic, that is the energy (expressed here as the electrochemical potential) required to convert iron oxide to iron decreases with increasing temperature. The range of 500 to 950 °C provides an ideal range for the electrolysis to occur at low potential and without the materials constraints and instabilities imposed by higher temperature operating conditions. We had recently discovered that the lithiation of iron oxides facilitates their concentrated dissolution in molten carbonates.

Both hematite, Fe_2O_3, and magnetite, Fe_3O_4, are highly soluble in molten lithiated carbonates.[1,11] We have observed a high solubility for both lower temperature eutectic carbonate melts ($Li_{0.87}Na_{0.63}K_{0.50}CO_3$), and for pure Li_2CO_3, (pure Li_2CO_3 melts at 723°C). In Li_2CO_3, ferric, [Fe(III)], solubility increases from 7 to 12 molal (molal = m ≡ moles per / kg Li_2CO_3) with temperature increase from 750 to 900°C, while in the eutectic the solubility increases from 1 to 4 m Fe(III) as temperature increases from 550°C to 900°C.

Lithium oxide is not consumed in the iron making process. For Fe_2O_3 in molten carbonate, the STEP iron production mechanism is given by:[1]
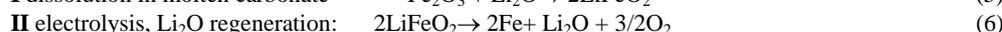
I dissolution in molten carbonate	$Fe_2O_3 + Li_2O \rightarrow 2LiFeO_2$	(5)
II electrolysis, Li_2O regeneration:	$2LiFeO_2 \rightarrow 2Fe + Li_2O + 3/2 O_2$	(6)
III net reaction, same as equation 3.		

Figure 1 compares conventional carbothermal, and STEP's electrolytic lithiated carbonate production of iron. Iron electrolysis, equations 3 and 4, are endothermic; higher temperature requires significantly less electrolysis energy. As previously studied, in the STEP processes this thermal energy is provided by concentrated sunlight leading to high solar energy conversion efficiencies. The measurements here focus on the electrochemical, rather than solar (which has been previously studied[1]), characterization of STEP Iron. A maximum coulombic efficiency, and a minimum electrolysis potential, are critical to the viability of the STEP Iron process, and have not been previously determined. This study probes that critical optimization for the electrolytic synthesis of iron metal from Fe_2O_3.
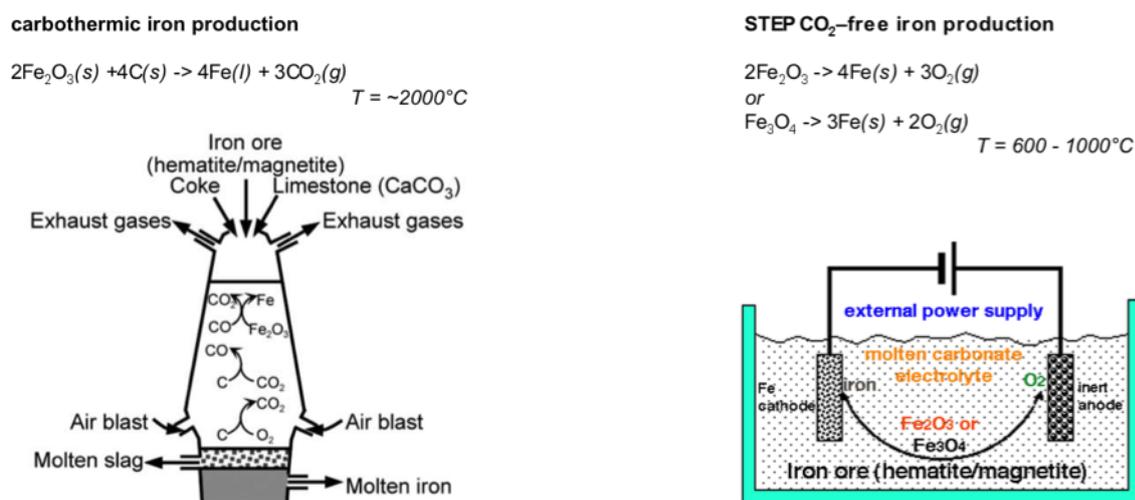
Figure 1. Comparison of the industrial (left) (left) and the STEP CO_2 free production of iron (right).

Experimental

Chemicals and Materials. Lithium carbonate utilized is (Li_2CO_3, Alfa Aesar, 99%), as well as ferric oxide, Fe_2O_3 (99.4%, JT Baker), Li_2O (Alfa 99.5%), 1mm and 2 mm Ni wire (Alfa 99.5 %) and Ni foil (McMaster pure Ni 200 shim), crucibles: nickel (VWR AA35906-KY), Fe wire (Anchor dark annealed annealed), steel foil (McMaster 75 μm 316 steel), crucibles: nickel (VWR AA35906-KY), high purity alumina (AdValue Technology AL-2100), silicon dioxide (SiO_2, Spectrum, 325 mesh), lithium orthosilicate is (Li_4SiO_4, Alfa Aeasar, 99.9%), Pflatz & Bauer, 99%).

Electrolyses. Electrolysis conditions and the systematic variation of the electrolysis cell components are described in the Systematic Optimization of electrolytic iron production in molten carbonate section. The theoretical maximum mass of iron that can be produced from the ferric salt during the electrolysis is calculated as Electrolysis current (A) x Electrolysis time (s) x Atomic Weight Fe / (3 e- x 96,485 As).

Analyses. Iron metal is produced by electrolysis in molten carbonate at the cathode. The cathode product is analyzed for iron metal content based on, and improved from the method of Xu and co-workers in which iron metal replaces cupper sulfate, and the product ferrous sulfate is analyzed.[13] The procedure has been further improved by (i) washing the electrolysis product with deionized water, and (ii) replacement of the previous UV/Vis evaluation which was used at the end of the procedure, with a more quantitative (less prone to colorimetric interference) titration by dichromate. The initial rinse removes Li_2CO_3 and Li_2O to prevent reaction of Fe^0 to form $Fe(OH)_2$ or $Fe(OH)_3$.

In addition to the relative valence state composition of iron, the mass percent of total iron in the sample (including the solidified electrolyte) is shown in the Fe_{total} of column in Table 1, and the last two columns are measured water soluble and water insoluble mass percent of each sample. The washed, dried insoluble component consists primarily of iron (iron metal and iron oxides). The iron analysis of weighed samples from each layer yields the concentrations: $[Fe_{total}]$, $[Fe°]$, $[Fe^{2+}]$, and $[Fe^{3+}]$ (the latter concentration is determined from the difference of $[Fe_{total}]$- $[Fe°]$- $[Fe^{2+}]$). A separate, weighed sample from each layer is washed, followed by subtraction of the mass of the dried insoluble (filtered, dried) component. This yields the mass of the remaining soluble components. The water soluble salts components consist of Li_2CO_3 and Li_2O. The Li_2O dissolves as LiOH, including Li_2O stripped from lithiated iron oxides when brought in contact with the wash water (*e.g.* $LiFeO_2 + H_2O$ liberates soluble LiOH), and the 105°C dried components are weighed as the insoluble salts).

The analysis procedure for iron metal is:

1) The cathode product is ground in a mortar and pestle, until it can be sifted and dispersed through a 70 mesh (212 μm) sieve.

2) The ground product is washed with deionized water, then extracted by suction filtration and rinsing the precipitate with deionized water until pH is near 7. The precipitates, residue and filter paper are collected to react with $CuSO_4$.

3) To 0.5 g of the ground product is added 50 ml of 0.5 M $CuSO_4$, to form:

$$Fe + CuSO_4 \rightarrow FeSO_4 + Cu \qquad (7)$$

4) After boiling this stirred solution for 1 hour, it is immediately filtered (to prevent the reaction of O_2 with Fe^{2+}) with a GF /A (Whatman glass microfiber) filter paper into a 250 ml volumetric flask, and the filter paper is washed with double deionized (18 MΩ) water also into the flask, and diluted to 250 ml.

5) 25 ml of the 250 ml filtrate is sampled by pipette into a 250 ml erlenmeyer flask,

and the following solutions are added to the flask: 20 ml of "A", 20 ml of "B", 50 ml of water, and 3 drops of indicator solution "C", where

A: is a mix of 50 ml of water with 10 ml concentrated H_2SO_4

B: 700 ml of water with 150 ml concentrated H_2SO_4, 150 ml H_3PO_4 (binds colored Fe^{3+}, which is colored, as colorless $Fe(HPO_4)_2^-$, to improve clarity of the endpoint)

C: Is the indicator solution consisting of 0.2% aqueous Diphenlyamine 4-sulfonic acid sodium salt

D: Is the titrant consisting of 0.004167 M (6 x dilution of 0.025 M) $K_2Cr_2O_7$

which tritrates as 1 equivalent $K_2Cr_2O_7$ per $FeSO_4$; each ml of solution D = 1.3962 mg of Fe° metal.

$$6FeSO_4 + K_2Cr_2O_7 + H_2SO_4 \rightarrow 3Fe_2(SO_4)_3 + K_2SO_4 + Cr_2(SO_4)_3 + 7H_2O \qquad (8)$$

The endpoint is observed as a color change from light blue (initial) to the endpoint's purple.

This titration analysis is also confirmed by weighing the mass of magnetically removed the iron product that was washed & dried to remove oxide. The reliability of the analysis during the titration is improved when solutions are stirred slowly in step 2, rather than rapidly, to prevent significant errors (underestimating the Fe° content of the product with increasing speed of stirring) due to the introduction of oxygen, which can convert ferrous to ferric prior to the titration. The need to switch to a lower stirring speed for the Fe° analysis was discovered and applied to the latter half of the experiments in this study. Under this latter condition replicate analyses of Fe° metal mass from are reproducible to within a $\pm 2\%$.

The analysis procedure for total Fe is:

In accord with the method of Shi et al,[14] a 0.1g sample was placed in a 250 ml flask with the addition of 20 ml of 1:1 diluted HCl. The sample was placed on a mixer hot plate at about 90 ^oC (to prevent volatile loss of $FeCl_3$ at higher temperature) until completely dissolved. 20 ml water was added under N_2 (99.999%). Al powder was added in three 0.1 g portions (in large excess of the theoretical amount to reduce Fe^{3+} to Fe^{2+}). With a minimum of stirring, the Al quickly reacts with Fe^{3+} and H^+ to form Al^{3+}, and Fe^{3+} was reduced to Fe^{2+}. A color change from yellow to light yellow was observed until the solution was transparent. The analysis occurs in accord with the following equations:

$$Al + Fe^{3+} \rightarrow Al^{3+} + Fe \qquad (9)$$
$$Fe + 2H^+ \rightarrow Fe^{2+} + H_2 \qquad (10)$$
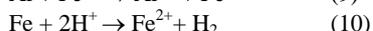
100 ml of H_2O was added and the solution was cooled until room temperature. 20 ml sulfuric-phosphoric acid solution and 5 drops of the diphenylamine indicator where added after which the solution was titrated with the standard $K_2Cr_2O_7$ solution (0.0250 mol 1/6 $K_2Cr_2O_7$/L).

Total Fe^{3+} (%) = V×N× FW Fe ÷1000/S

V-- standard $K_2Cr_2O_7$ solution volume, ml.

N-- standard $K_2Cr_2O_7$ solution concentration, mol/L.

FW Fe = 55.85 g/ mol.

S—specimen weight, g.

The analysis procedure for Fe^{2+} is based on the method of reference 14, as modified by references 13 and 15. In this analysis, 0.5 g of the sample to be analyzed was added to 250 ml flask and 20 ml of 1:1 diluted HCl was added. This solution was mixed on a hot plate under 99.999% N_2 at 90 ^oC until completely dissolved. 100 ml H_2O was added and the solution allowed to cool to room temperature. 20 ml sulfuric-phosphoric acid solution (prep: add 600 ml concentrated H_2SO_4 to 800 ml stirred DI, then add 600 ml of 86% phosphoric acid) and 5 drops of the diphenylamine indicator were added and titrated with the standard $K_2Cr_2O_7$ solution (0.0250 mol 1/6 $K_2Cr_2O_7$/L) to a sharp endpoint color change from green to purple.

In accord with the equation:

Fe^{2+} (%) = V×N×FW Fe÷1000/S.

V-- standard $K_2Cr_2O_7$ solution volume, ml.

N-- standard $K_2Cr_2O_7$ solution concentration, mol/L.

S—specimen weight, g.

The analysis procedure for Fe^{3+} is the straightforward difference from the known total iron, the sum of the iron metal and ferrous species as: Fe^{3+}(%)= Total Fe(%)-Fe^0 (%)-Fe^{2+} (%)

The analysis procedure for the aqueous soluble components:

Filters were dried in an oven at 105 °C for 1 hour, and then cooled in a desiccator, and weighed. After weighing, samples (~0.3g) to be analyzed were stirred one hour in 100 ml of DI (18 MΩ) in a 250 ml flask at room temperature, then filtered using suction, and the filtrate washed on the filter with three 20 mL volumes of DI water. The filter is transferred onto a glass weighing dish, and dried 105°C for a minimum of 1 hour until a minimum mass is measured (after cooling to room temperature in the desiccator).

Equation: Water soluble substances (wt%) = (A-B)×100/A.

A—Specimen weight, g.

B-- Residue on the filter paper weight, g.

Systematic Optimization of electrolytic iron production in molten carbonate.

A systematic, variation of molten iron electrolysis can yield efficient iron production efficiency at low energy. General conditions of the first series of electrolyses are summarized in Table 1. The cathode in this first series of experiments is a thin planar 6.25 cm^2 steel sheet. This cathode lies under the anode, and we observe that the iron product is deposited on top of the cathode. This cathode surface is the active area exposed to short ion diffusion path between the electrodes.

Table 2 summarizes the results of 1 hour electrolyses at 1 Amp in an 800°C molten lithium carbonate electrolyte containing 1.5 m Fe_2O_3 and 3 m Li_2O (to generate 3 m $LiFeO_2$ in solution). In this series of experiments the anode, a coiled pure nickel (McMaster 200 Ni) wire is situated 3 mm below the surface of the electrolyte to facilitate oxygen evolution in an attempt to minimize oxygen interaction with the cathode product.

Table 1. Constant characteristics in the first series of STEP Iron parametric optimization studies.

Current of electrolysis	1.0 amp
Time of electrolysis (1h)	3600 s
Theoretical max mass Fe^0 from electrolysis: $Fe^{3+}+3e^- \rightarrow Fe^0$	$1A \times 3600 \div 96485 \div 3 \times 55.85 = 0.696$ g
Anode: Ni wire tightly coiled, l = 16 cm, d = 2.0 mm, area:	10 cm^2
Cathode: Steel shim, 2.5cm$\times$2.5cm, area	6.25 cm^2

Figure 2. Anode (upper electrode) and cathode (lower electrode) prior to electrolysis (top) and following electrolysis prior to removal of cathode product (bottom). Insulating alumina ceramic tubes are reused and hence appear charred.

In the first series of experiments, summarized in Table 2, the anode to interelectrode spacing is varied, and the mass of electrolyte was changed to cover smaller or larger inter-electrode separations. The electrodes before and after electrolysis are photographed in Figure 2. The lithium based electrolyte is highly conductive, and even at these relatively high current densities, electrolytic resistance losses are not significantly impacted by the variation of inter-electrode spacing. The electrolysis potentials at 1 A constant current are the same to within 0.1 V, independent of the 0.25 to 2.0 cm electrode separation. Coulombic efficiency, particularly during the 0.25 cm separation electrolysis may have been impacted by shorting as the iron deposit growing from the cathode approached the anode, and that a maximum of over 50% coulombic efficiency is achieved for an intermediate spacing of 1.0 cm.

Table 3 summarizes STEP Iron electrolyses in which the starting concentration of Li_2O is varied. In each case, the initial ferric concentration (as added Fe_2O_3) is kept constant at 3 molal Fe^{3+} in Li_2CO_3. As we have previously demonstrated, Fe_2O_3 is not soluble in carbonate unless Li_2O is added, and reacts to form $LiFeO_2$ in the molten solution.[1] The Li_2O is not consumed in the electrolysis process. That is consistent with eq. 7, as $LiFeO_2$ is reduced to form iron metal, Li_2O is liberated to dissolve the next iteration of added iron ore (Fe_2O_3). As seen in the photo in Figure 3, the iron is deposited directly on top of the cathode, followed by a black layer of partially reduced iron (magnetite), followed by a layer of the electrolyte containing the excess (brown) Fe_2O_3 dissolved in the electrolyte. The iron layer is easily separated from the cathode, Figure 4, and as seen in Figures 3 and 4 leaves behind a reusable cathode. As seen in Table 3, a 1:1 ratio of Li_2O to Fe_2O_3 supports the maximum coulombic efficiency, although it is interesting to note in Figure 5, that higher concentrations of Li_2O significantly decrease the required electrolysis potential (as seen comparing the 1.5 m and 9.0 m Li_2O electrolysie). This decrease in potential with increasing oxide concentration may be due to the formation of a peroxoide intermediate in the anodic evolution of oxygen as we have recently demonstrated.[11] Also evident in the figure, potential variations are occasionally observed during individual electrolyses, although average electrolysis potential trends are highly consistent.

Table 2. Effect of electrode spacing and electrolyte mass on electrolysis. Electrodes are delineated in Table 1. The electrolyte mass was changed as indicated below, to maintain electrolyte converage in experiments with smaller or larger inter-electrode separations. Note, coulombic efficiency, particularly during the 0.25 separation electrolysis may have been impacted by shorting as the iron deposit grew from the cathode towards the anode.

Temperature (^{o}C)	800	800	800	800
Anode/Cathode separation (cm)	0.25	0.5	1.0	2.0
Electrolyte Total mass (g): Electrolyte weighed from a mix of 200.0015g Li_2CO_3, 47.8888g Fe_2O_3 and 17.9286g Li_2O,	8.3193	16.6128	33.2174	66.4510

Fe^{3+} concentration (mol /kg Li_2CO_3) as Fe_2O_3	3.0 m	3.0 m	3.0 m	3.0 m
Li_2O concentration (mol /kg Li_2CO_3)	3.0 m	3.0 m	3.0 m	3.0 m
Cathode: Steel shim, 2.5cm×2.5cm	6.25 cm²	6.25 cm²	6.25 cm²	6.25 cm²
Fe^0 mass in product (g)	0.135	0.328	0.381	0.249
Coulombic efficiency (100%x Fe^0 mass experiment/theory)	19.4	47.0	54.7	35.7

The next series of experiments utilizes the general conditions described in Table 2, still at constant (1.0 amps) current, but varies the electrolysis time. As summarized in Table 4, whereas 1 hour of electrolysis should theoretically yield 0.7 g of iron (assuming 1000% coulombic efficiency of the three electron reduction of dissolved Fe^{3+}), 8 hours of electrolysis would be expected to generate 5.6 g of iron metal. As summarized in Table 4, the experimental coloumbic efficiency during electrolysis is approximately 50 percent and is not substantially affected by the electrolysis time. What is affected, as shown in the photos in Figure 6, is the amount of salt that is removed with the product, and is enriched 5-fold in iron metal after the extended electrolysis. The amount of salt accompanying the cathode product is seen to be much lower after 8h electrolysis than after 1 hour electrolysis. In each case, the cathode product is washed prior to the iron(0) content analysis. Even subsequent to extended electrolysis time, each of the cathodes remain intact after the removal of product. As seen in Figure 6, the 8 hour electrolysis cathode product does not exhibit the multiple layers evident, and instead has iron metal throughout the product (but the iron remains spatially diffuse intermingled with electrolyte).

Table 3. Effect of Li_2O concentration on electrolysis. The anode/cathode separation is 1.0 cm; other electrolysis conditions are detailed in Table 1. Note, an intermediate Li_2O concentration (2 molal) conducted for double the electrolysis time, generated greater iron metal product.

Temperature (°C)	800	800	800	800
Time of electrolysis (h) at 1.0 amp	*1h*	**2h**	*1h*	*1h*
Theoretical max mass Fe^0 from electrolysis: $Fe^{3+} + 3e^- \rightarrow Fe^0$	0.696 g	1.389 g	0.696 g	0.696 g
Average Potential of electrolysis (V)	1.84	1.80	1.69	1.57
Carbonate Electrolyte: Li_2CO_3 (g)	25.000	25.001	24.992	21.999
Fe^{3+} concentration (mol /kg Li_2CO_3)	3.0 m	3.0 m	3.0 m	3.0 m
Fe_2O_3 mass (g)	5.9866	5.9868	5.9843	5.9167
Li_2O concentration (mol /kg Li_2CO_3)	1.5 m	**2.0 m**	**3.0 m**	**9.0 m**
Li_2O mass (g)	1.1200	1.4941	2.241	5.9167
Electrolyte Total Weight (g)	32.1138	32.4217	33.2174	33.1841
Fe^0 mass in product (g)	0.312	0.711	0.381	0.155
Coulombic efficiency (100%x Fe^0 mass exper/theory)	44.8	51.7	54.7	22.3

Figure 3. Side view of cathode with product.
Figure 4. Cathodes, after removal of product, remain intact.
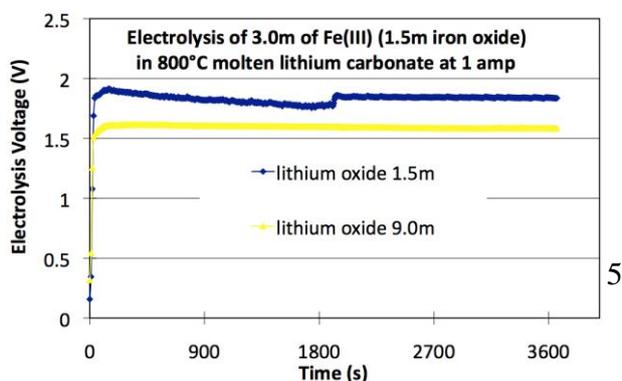
Figure 5. Variation of STEP Iron electrolysis potential with different Li_2O concentrations.

5

Sodium carbonates (mp 851°C) or potassium carbonate (mp 891°C) both have higher melting points than lithium carbonate (mp 723°C). However, a eutectic mix of the three carbonates, such as $Li_{0.85}Na_{0.61}K_{0.54}CO_3$, has melting point below 400°C, and provides an opportunity to explore STEP Iron at lower temperatures. At these lower temperature conditions, the electrolysis potential would be expected to be considerably higher. As previously shown the reaction of iron oxide to iron and oxygen is endothermic, with (i) an increase in rest potential with decrease in temperature. This will be exacerbated by (ii) a lower solubility of iron oxide in the eutectic at lower temperature and with lower lithium ion content, and (iii) higher overpotential due to the higher electrolyte resistance of a mixed alkali, compared to pure lithium, electrolyte. The general conditions of electrolysis are similar to those in Table 1. At the lower 500°C temperature, only a lower concentration of iron oxide could be dissolved in the eutectic and the sustainable current at a reasonable electrolysis potential was only, 0.4 A, rather than 1A. Hence, the electrolysis time was increased from 1 to 2.5 hours to provide a constant total current during the experiment. As summarized in Table 5, even at the lower current, the lower temperature still requires a high (3.5V) average electrolysis potential, and results in a poor coulombic efficiency. As seen in Table 5, by 750°C, the $Li_{0.85}Na_{0.61}K_{0.54}CO_3$ eutectic could readily accommodate the full 3 molal Fe^{3+} used in the pure lithium carbonate electrolyte at 800C. It is evident in the figure that in the eutectic at 750C, a higher electrolysis potentials was needed to accommodate the same 1 Amp current used in the pure lithium electrolyte. Interestingly, coulombic efficiencies are high in both cases, and as seen in Figure 7, the cathode product contains a low fraction of removed salt, and a high fraction of iron.

Table 4. Effect of electrolysis time on the electrolytic formation iron. The anode/cathode separation is 1.0 cm; other electrolysis conditions are detailed in Table 1.

Temperature (°C)	800	800	800	800	800
Time of electrolysis (h) at 1.0 amp	*1h*	**1h 20m**	**2h**	**4h**	**8h**
Theoretical max mass Fe^0 via: $Fe^{3+}+3e^- \rightarrow Fe^0$	0.696 g	0.926 g	1.389 g	2.778 g	5.557 g
Average Potential of electrolysis (V)	1.69	1.75	1.57	1.7	1.65
Fe^{3+} concentration (mol /kg Li_2CO_3) as Fe_2O_3	3.0 m	3.0 m	3.0 m	3.0 m	3.0 m
Li_2O concentration (mol /kg Li_2CO_3)	3.0 m	3.0 m	3.0 m	3.0 m	3.0 m
Electrolyte Total Weight (g)	33.2174	33.0001	33.2163	33.2143	33.2177
Fe^0 mass in product (g)	0.381	0.529	0.732	1.493	2.553
Coulombic efficiency (100%x Fe^0 mass exp/theory)	54.7	57.1	52.7	53.7	45.9
* = anode contact broke just prior to completion		*	*		

Figure 6. Product removed and partially peeled from cathode after 1 or 8 hour electrolyses. The amount of salt removed with the product is high after 1h electrolysis (then washed prior to analysis) & lower after the extended (8h) electrolysis. During the 8h electrolysis, a higher fraction of the initial 3 m of Fe^{3+} is converted to Fe' & the product layer sitting on the cathode is enriched in iron metal.

Figure 7. (right) Side view of cathode with product after 1h 3 m $LiFeO_2$ in $Li_{0.85}Na_{0.61}K_{0.54}CO_3$ 750°C STEP iron electrolysis.

Table 5. Effect of eutectic ($Li_xNa_yK_zCO_3$) or pure (Li_2CO_3) carbonate, and of temperature, on the electrolytic formation iron. The electrodes are separated by 1.0 cm and are detailed in Table 1.

Temperature (°C)	**500**	**750**	**800**
Time of electrolysis (h)	*2.5h*	*1h*	*1h*
Electrolysis current (A)	0.4	1.0	1.0
Average Potential of electrolysis (V)	3.5	1.95	1.69
Carbonate Electrolyte	$Li_{0.85}Na_{0.61}K_{0.54}CO_3$	**$Li_{0.85}Na_{0.61}K_{0.54}CO_3$**	**Li_2CO_3**
Carbonate Electrolyte: Li_2CO_3 (g)	30.0026	25.0002	24.9926
Fe^{3+} concentration (mol /kg Li_2CO_3)	0.8 m	3.0 m	3.0 m
Fe_2O_3 weight (g)	1.9156	5.9861	5.9843
Li_2O concentration (mol /kg Li_2CO_3)	0.8 m	3.0 m	3.0 m
Li_2O weight (g)	0.7177	2.2416	2.241
Electrolyte Total Weight (g)	32.6468	33.2349	33.2174
Fe^0 mass in product (g)	0.026	0.388	0.381
Coulombic efficiency (100%xFe^0 mass exp/theory)	3.73	55.8	54.7

Table 6. Effect of planar foil cathode surface area on the electrolytic formation iron. The electrolysis time, current, theoretical maximum mass of iron, and anode are as detailed in Table 1. Inter-electrode separation is 1.0 cm. Cathodes are described in the table.

Temperature (^{o}C)	800	800	800	800
Average Potential of electrolysis (V)	1.66	1.68	1.69	1.43
Electrolyte Total Weight (g): Electrolyte weighed from a mix of 200.0015g Li_2CO_3, 47.8888g Fe_2O_3 and 17.9286g Li_2O,	33.2161	33.2093	33.2174	33.281
Fe^{3+} concentration (mol /kg Li_2CO_3) as Fe_2O_3	3.0 m	3.0 m	3.0 m	3.0 m
Li_2O concentration (mol /kg Li_2CO_3)	3.0 m	3.0 m	3.0 m	3.0 m
Cathode: Steel shim, 2.5cm×2.5cm	0.8 cm^2	**2.5 cm^2**	**6.25 cm^2**	**12.5 cm^2**
Fe^0 mass in product (g)	0.238	0.325	0.381	0.191
Coulombic efficiency (100%x Fe^0 weight experiment/theory)	34.2	46.7	54.7	27.5

Table 6 summarizes interesting, but unsuccessful, attempts to improve the coulombic efficiency of the planar iron foil cathode, by increasing or decreasing its surface area. As seen in Figure 8, two smaller surface area electrodes were compared, as well as a double surface area electrode folded in an accordion configuration to accommodate the double width of the electrode. As summarized in Table 6, while the larger surface area electrode did decrease the average electrolysis potential, the coulombic efficiency was maximum for the simpler planar, solid cathode. As in prior experiments, the anode was a Ni coil, 16 cm length, 2.0 mm diameter, area 10 cm^2, and the anode/cathode inter-electrode separation was 1 cm.

Figure 8 (left). Solid steel foil cathodes with various surface areas prior to electrolysis (top) and following electrolysis with partial removal of cathode product (bottom). Spot welds to connect the steel wire contacts are evident.

Figure 9. The 6.25 cm^2 foil, and 5 or 20 cm^2 coiled wire, cathodes prior to electrolysis.

   Table 7 summarizes a successful attempt to modify the cathode configuration, which is accomplished by transitioning from a planar, to a coiled, steel cathode. Figure 9 compares the planar and coiled cathode configurations. Not shown is the similar, intermediate 10 cm^2 coil, which appears to combine the advantages of a loose coil packing with a relatively high surface. Interpolating between the coulombic efficiencies of the 5 or 10 cm^2 coiled cathodes, it can be noted that the 6.25 cm^2 foil cathode exhibits similar efficiencies to the same surface area coiled wire electrode. A common impurity in iron ores is silicate. Another change in this experiment was addition of 10%, by mass, lithium silicate as an initial attempt to simulate the electrolysis of iron ore with silicate. As seen comparing Tables 6 and 7, the silicate marginally diminishes the coulombic efficiency at the planar, foil electrode to 51%. However, the coulombic efficiency at the 10 cm^2 coiled steel wire cathode is higher at 55%.

Table 7. Effect of cathode shape and current density (determined by cathode surface area) on the electrolytic formation of iron. The anode, with an anode/cathode separation of 1.0 cm is detailed in Table 1. Cathodes are described in the table. Each electrolysis is at 1 A for 2 hours.

Temperature (^{o}C)	800	800	800	800
Average Potential of electrolysis (V)	1.636	1.759	1.787	1.738
Carbonate Electrolyte: Li_2CO_3 (g)	25.0	25.0	25.0	25.0
Fe^{3+} concentration (mol /kg Li_2CO_3)	3.0	3.0	3.0	3.0
Fe_2O_3 weight (g)	5.9885	5.9886	5.9880	5.9883
Li_4SiO_4 (g) (10 wt % SiO_2 content in Fe_2O_3)	1.194	1.194	1.194	1.194
Electrolyte Total Weight (g)	33.9996	34.0005	34.4254	34.0002

Cathode: Area (cm^2)	6.25	**5.0**	**10.0**	**20.0**
Size: Length×width or diameter (cm) Shape: foil or coiled wire	2.5×2.5 Fe foil	13.3×0.12 Fe wire	26.5×0.12 Fe wire	53×0.12 Fe wire
Current density (mA/cm^2)	160	**200**	**100**	**50**
Fe^0 mass in product (g)	0.7049	0.2994	0.7693	0.6350
Coulombic efficiency (100%x Fe^0 weight experiment/theory)	51%	22%	55%	46%

In the absence of silicate, the improvement in coulombic efficiency with the larger surface area coiled, rather than smaller surface area planar, cathode is more evident. Table 8 summarizes results of electrolyses each using a 10 cm^2 coiled cathode, and with either 2, 3, 4 or 6 molal Fe^{3+}, and Li$_2$O in 800°C molten lithium carbonate. The coulombic efficiency is high and comparable in the 3 and 4 molal electrolytes, with the 3 molal exhibiting a modestly higher efficiency of 70%. In the presence of 10% silicate, as seen in Table 9, and continuing with use of the preferred coiled cathode, the coulombic efficiency is somewhat higher in the 3, rather than 2, molal Fe^{3+}, and higher when a 1:1 equivalent ratio, rather than a 2:1 equivalent ratio of Li$_2$O is used. In all cases the presence of the silicate decreases the measured coulombic efficiency.

Table 8. Effect of Fe$_2$O$_3$ concentration on the electrolytic formation iron. The anode is as detailed in Table 2, with an anode/cathode separation of 1.0 cm. Cathodes are described in the table. Each electrolysis is at 1 A for 1 hour.

Temperature (°C)	800	800	800	800
Average Potential of electrolysis (V)	1.6645	1.826	1.847	1.584
Carbonate Electrolyte: Li$_2$CO$_3$ (g)	26.9996	25.0006	23.0006	21.0003
Fe^{3+} concentration (mol /kg Li$_2$CO$_3$)	2.0	**3.0**	**4.0**	**6.0**
Fe$_2$O$_3$ weight (g)	4.3117	5.9881	7.3460	10.0603
Li$_2$O concentration (mol /kg Li$_2$CO$_3$)	2.0	3.0	4.0	6.0
Li$_2$O weight (g)	1.6134	2.2413	2.7485	3.7643
Electrolyte Total Weight (g)	32.9352	33.2002	33.0226	34.8159
Cathode: Fe coil, 26.5 cm length, 1.2 mm diameter, area	10 cm^2	10 cm^2	10 cm^2	10 cm^2
Fe^0 mass in product (g)	0.7229	0.9710	0.9496	0.4111
Coulombic efficiency (100%x Fe^0 weight experiment/theory)	52%	70%	68%	30%
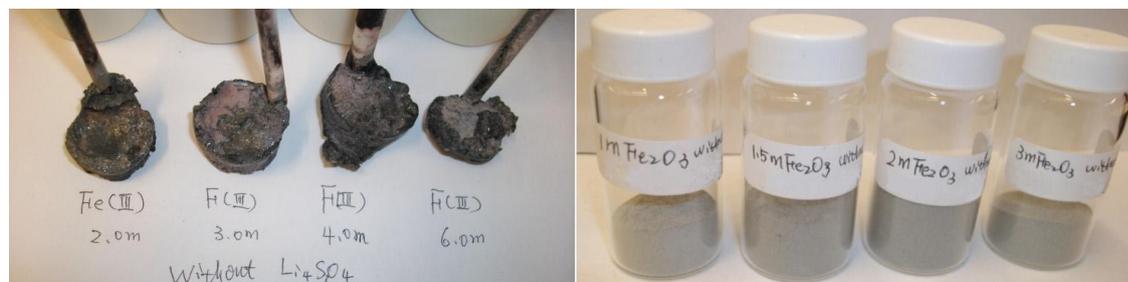
Figure 10. Left: 10 cm^2 coiled steel foil cathodes removed after the electrolyses described in Table 8. Right: removed, then ground product, prior to washing from the electrodes picture on the left side.

Table 9. Effect of Fe$_2$O$_3$ concentration in an electrolyte containing dissolved silicate (10 wt % SiO$_2$ content in Fe$_2$O$_3$), on the electrolytic formation of iron. The anode is as detailed in Table 1, with an anode/cathode separation of 1.0 cm. Cathodes are described in the table. Each electrolysis is at 1 A for 2 hours.

Temperature (°C)	800	800	800	800
Average Potential of electrolysis (V)	1.639	1.791	1.791	1.745
Carbonate Electrolyte: Li$_2$CO$_3$ (g)	26.9992	24.9994	22.9998	20.9994
Fe^{3+} concentration (mol /kg Li$_2$CO$_3$)	**2**	**3**	**2**	**3**
Fe$_2$O$_3$ mass (g)	4.3115	5.9886	7.3468	10.0603
Li$_2$O concentration (mol /kg Li$_2$CO$_3$)	2	3	4	6
Li$_2$O weight (g)	1.6132	2.2411	2.7485	3.7648
Li$_4$SiO$_4$ (g) (10 wt % SiO$_2$ content in Fe$_2$O$_3$)	**0.8605**	**1.1942**	**1.4659**	**2.0068**
Electrolyte Total Weight (g)	33.7870	34.4254	34.5667	36.8151

Cathode: Fe coil, 26.5 cm length, 1.2 mm diameter, area	10 cm^2	10 cm^2	10 cm^2	10 cm^2
Fe^0 mass in product (g)	0.6708	0.7693	0.4784	0.5899
Coulombic efficiency (100% x Fe^0 weight experiment/theory)	48%	55%	34%	42%

Table 10 summarizes probes of the temperature effect on STEP Iron electrolysis in a pure lithium carbonate electrolyte (but containing silicate, and 3 molal Fe^{3+} and Li$_2$O). While the electrolysis potential decreases with increasing temperature, the electrolysis efficiency is lowest (23%) at the highest, 900°C, temperature, and highest (58%) at the lowest, 750°C, electrolysis temperature. The lower efficiencies, at higher temperature, may be associated with the greater reactivity and diffusivity of the oxygen produced at the anode, which can back react with iron to form a parasitic iron oxide loss. Table 11 further probes of silicate effect on STEP Iron. We had previously studied the dissolution of silica, SiO$_2$, as Li$_4$SiO$_4$ in molten carbonates.[11] Here, we see the trend that higher SiO$_2$ ranging from 10 to 30% (added as a percentage of the iron oxide mass to simulate an impurity in the iron ore), tends to decrease the average electrolysis potential, but also decreases the coulombic efficiency of iron production.

Table 10. Effect of temperature on the 1 A, 2 hour electrolytic formation iron (with silicate in electrolyte). The anode, detailed in Table 2, is separated from the cathode by 1.0 cm.

Temperature (°C)	**750**	**800**	**900**
Average Potential of electrolysis (V)	1.801	1.788	1.522
Carbonate Electrolyte: Li$_2$CO$_3$ (g)	25	25	25
Fe^{3+} concentration (mol /kg Li$_2$CO$_3$)	3	3	3
Li$_2$O concentration (mol /kg Li$_2$CO$_3$)	3	3	3
Li$_4$SiO$_4$ (g	1.194	1.194	1.194
Electrolyte Total Weight (g)	33.9999	34.4254	33.9998
Cathode: Fe coil, 26.5 cm length, 1.2 mm diameter. area	10 cm^2	10 cm^2	10 cm^2
Fe^0 mass in product (g)	0.8067	0.7693	0.3183
Coulombic efficiency (100% x Fe^0 weight experiment/theory)	58%	55%	23%

Table 11 . Effect of SiO$_2$ content on the 1 A, 2 hour electrolytic formation iron. Anode/cathode separation is 1.0 cm; anode as detailed in Table 1.

Temperature (°C)	800	800	800
Average Potential of electrolysis (V)	1.794	1.812	1.672
Carbonate Electrolyte: Li$_2$CO$_3$ (g)	24.9994	25.0000	24.9996
Fe^{3+} concentration (mol /kg Li$_2$CO$_3$)	3	3.0	3.0
Fe$_2$O$_3$ weight (g)	5.9886	5.9880	5.9883
Li$_2$O concentration (mol /kg Li$_2$CO$_3$)	3.0	3.0	3.0
Li$_2$O weight (g)	2.2411	2.241	2.2410
Li$_4$SiO$_4$ (g) = Fe$_2$O$_3$ weight × SiO$_2$ content ÷ 60.08 (SiO$_2$) × 119.84(Li$_4$SiO$_4$)	1.1942	1.7940	3.5883
SiO$_2$ content in Fe$_2$O$_3$ (wt %)	**10%**	**15%**	**30%**
Cathode: Fe coil, 26.5 cm length, 1.2 mm diameter, area	10 cm^2	10 cm^2	10 cm^2
Fe^0 mass in product (g)	0.7693	0.7282	0.5668
Coulombic efficiency (100% x Fe^0 weight experiment/theory)	55%	52%	41%

In the next series of experiments the anode stability was improved by raising the anode, from 3 mm below the electrolyte surface (a configuration used in all prior experiments), up to the surface of electrolyte. Prior to this surface anode configuration, anodes occasionally spontaneously broke during the course of the electrolysis. However the surface anodes appear to be fully stable, that is, there is no case of anode discontinuity occurring with the surface anodes in the next 30 experiments, independent of electrolysis conditions, and the anode always appeared to be unaffected by the electrolysis (no corrosion was evident).

Table 12. Effect of surface area of the anode, when situated at the surface (the interface between the molten electrolyte and the gas above the melt), on the 1 A, 2 hour electrolytic formation iron. Anode and cathode are detailed below in the table.

Temperature (°C)	800	800	800	800	800

Anode: Ni wire, 2.0 mm diameter, length:	2 cm	8 cm	16 cm	16 cm	30 cm
surface area:	1.3 cm^2	**5 cm^2**	**10 cm^2**	**10 cm^2**	**18.8 cm^2**
coil configuration:	tight	tight	tight	loose	tight
Cathode: Fe coil, l = 26.5 cm, d =1.2 mm, area:	10 cm^2	10 cm^2	10 cm^2	10 cm^2	10 cm^2
Average Potential of electrolysis (V)	1.96	1.91	1.89	1.83	1.66
Fe^{3+} concentration (mol /kg Li$_2$CO$_3$) as Fe$_2$O$_3$	3.0 m	3.0 m	3.0 m	3.0 m	3.0 m
Li$_2$O concentration (mol /kg Li$_2$CO$_3$)	3.0 m	3.0 m	3.0 m	3.0 m	3.0 m
Electrolyte total mass (g)	33.2176	33.2167	33.2172	33.2172	33.2161
Li$_4$SiO$_4$ (g)	0	0	0	0	0
Fe^0 mass in product (g)	0.490	0.826	0.808	0.563	0.655
Coulombic efficiency (100%x Fe^0 mass exp/theory)	35.2	59.3	58.0	40.4	47.0

In Table 12 two anode parameters are varied, the surface area, and whether the anode wire is loosely or tightly coiled, as illustrated in the photographs of Figure 11. As seen in Table 12, the electrolysis potential decreases with increasing anode surface area, and its overpotential decreases by 300 mV as the surface area is increase from 1.3 to 19 cm^2. With the exception of the largest anode surface cell (which may be an outlier and exhibited an unstable electrolysis potential), the coulombic efficiency increases with increasing anode surface area, and the tightly coiled anode configuration leads to higher efficiency than the loosely coiled anode configuration. Finally, the surface anode in Table 12, while more stable operates at lower coulombic efficiency than its 10 cm^2 tightly coiled counterpart in Table 9.

Figure 11. Coiled nickel wire anodes with a tight or loose (open) prior to the Table 12 electrolyses.

Table 13 presents the effect of the gas above the electrolysis on the iron production, when the gas is changed from either air, to carbon dioxide, or to nitrogen. It is seen here that nitrogen significantly lowers the electrolysis potential and that both N$_2$ or CO$_2$ can improve the coulombic efficiency. As previously shown,[1] pure CO$_2$ will be absorbed in the electrolyte according to the back reaction of the lithium carbonate decomposition/reformation equilibrium. Air contains (0.03%) CO$_2$, and molten situated Li$_2$CO$_3$ below a blanket of air will be relatively stable, while pure N$_2$, without CO$_2$, will slowly decompose in accord with the equilibrium equation: Li$_2$CO$_3 \rightarrow$ CO$_2$ +Li$_2$O. Nitrogen above the electrolysis is seen to decrease the electrolysis potential, and has only a marginal impact on coulombic efficiency. As also summarized in Table 13, additional Li$_2$O added to the molten lithium carbonate electrolyte (above 3 m) decreases coulombic efficiency, but sustains the electrolysis at a lower potential.

Table 13. Effect of the gas above the melt, and the Li$_2$O concentration, on the electrolytic 1A, 2 hour formation of iron.

Temperature (^{o}C)	800	800	800	800	800
Gas above electrolyte	**air**	**air**	**CO$_2$**	**N$_2$**	**air**
Anode: Ni wire, 2.0 mm diameter, length:	16 cm	16 cm	16 cm	16 cm	16 cm
surface area:	10 cm^2	10 cm^2	10 cm^2	10 cm^2	10 cm^2
coil configuration:	tight	tight	tight	tight	tight
Cathode: Fe coil, l = 26.5 cm, d =1.2 mm, area:	10 cm^2	10 cm^2	10 cm^2	10 cm^2	10 cm^2
Average Potential of electrolysis (V)	1.87	1.80	1.95	1.62	1.71
Fe^{3+} concentration (mol /kg Li$_2$CO$_3$) as Fe$_2$O$_3$	3.0 m	3.0 m	3.0 m	3.0 m	3.0 m
Li$_2$O concentration (mol /kg Li$_2$CO$_3$)	**2.0 m**	**3.0 m**	3.0 m	3.0 m	**4.0 m**
Electrolyte total mass (g)	32.5140	33.2172	33.2153	33.2131	33.9994
Fe^0 mass in product (g)	0.880	0.808	0.871	0.833	0.708
Coulombic efficiency (100%x Fe^0 mass exp/theory)	63.17	58.0	62.5	62.8	50.8

Lowering the electrolysis temperature and decreasing the cathode current density can improve coulombic efficiency. As seen in Table 14, the columbic efficiency is increased by over 20%, that is to ~85%, by simultaneously decreasing the electrolysis temperature from 800°C to 750°C, and/or by increasing the cathode surface area. This is not observed when the temperature is held constant and the cathode surface area is decreased to 7.5 cm^2. Table 14 onward, are presented in an

abbreviated format, without the electrolyte concentration to save manuscript space. In each case the electrolyte total mass is ~ 33 g. In each case the electrolyte is 3.0 m in Fe^{3+} and Li_2O and without silicates. The coulombic efficiency also depends on when the electrode is removed from the electrolysis chamber (electrolysis time, Table 15) and the electrolysis current (Table 16). As seen in Table 15, removing the electrode after, 1 hour negatively impacts the efficiency, although this effect presumably may be mitigated if iron oxide is fed into the electrolysis chamber as iron is produced.

Table 14. Effect of the decrease in temperature and variation in cathode surface area on the 1A, 2 hour electrolytic formation of iron with coiled iron cathodes. The electrolyte is 3.0 m in Fe^{3+} and Li_2O.

Temperature (^oC)	750	**750**	750	**800**
Gas above electrolyte	**N₂**	**N₂**	**N₂**	**N₂**
Anode: Ni wire, d = 2.0 mm, l = 16 cm, coil, area:	$10\ cm^2$	$10\ cm^2$	$10\ cm^2$	$10\ cm^2$
Cathode: Fe coil, 1.2 mm diameter, length:	20 cm	26.5 cm	33 cm	26.5 cm
surface area:	$7.5\ cm^2$	**$10\ cm^2$**	$12.5\ cm^2$	**$10\ cm^2$**
Average Potential of electrolysis (V)	1.90	2.1	2.0	1.62
Coulombic efficiency (100%x Fe^0 mass exp/theory)	75.4	86.7	84.7	62.8

Table 15. Effect of the electrolysis time in a lower temperature (750 °C) lithium carbonate electrolyte on the electrolytic formation iron with coiled iron cathodes. The electrolyte is 3.0 m in Fe^{3+} and Li_2O.

Temperature (^oC)	750	750	750	750
Gas above electrolyte	**N₂**	**N₂**	**N₂**	**N₂**
Anode: Ni wire, d = 2.0 mm, l = 16 cm, coil, area:	$10\ cm^2$	$10\ cm^2$	$10\ cm^2$	$10\ cm^2$
Cathode: Fe coil, l = 26.5 cm, d =1.2 mm, area:	$10\ cm^2$	$10\ cm^2$	$10\ cm^2$	$10\ cm^2$
Time of electrolysis (h) at 1.0 amp	*1h*	*2h*	*3h*	*4h*
Coulombic efficiency (100%x Fe^0 mass exp/theory)	79.6	86.7	69.6	57.4
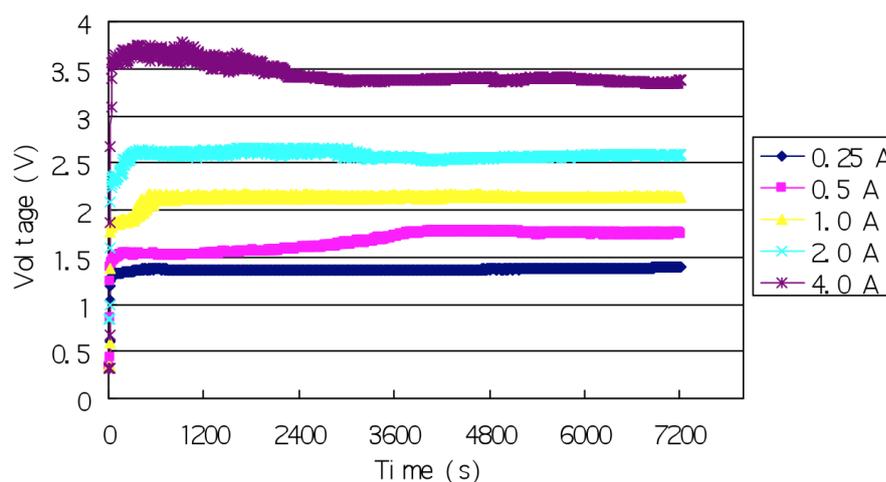
Figure 12. Variation of STEP Iron electrolysis potential with electrolysis current in a lower temperature (750 °C) lithium carbonate electrolyte.

Current density, Table 16, substantially effects the electrolysis with a maximum coulombic efficiency of 93% observed at 0.5 A, and as seen in Figure 12, a substantial decrease of the electrolysis potential at lower currents; a lowering of 2 volts between the electrolyses at 4.0 A compared to 0.25 A. A further increase in coulombic efficiency of the electrolytic formation of iron at 1 A occurs at even lower temperature, 730°C in Table 17. This temperature approaches the 723°C melting point of pure Li_2CO_3. While the efficiency falls rapidly at high temperature, the electrolysis potential is lower as seen in Figure 13. Electrolyte decomposition (from lithium carbonate to lithium oxide and carbon dioxide) occurs more rapidly at higher temperature. There is little decomposition at 750°C,[2] and the decomposition which occured at higher temperature may be controlled or eliminated by increasing the lithium oxide concentration within the electrolyte, or increasing the concentration of carbon dioxide in the atmosphere above the electrolysis. Hence, flowing air (0.03% CO_2), rather than nitrogen (0% CO_2), above the electrolysis will decrease the rate of electrolyte loss at higher temperature, even though as seen in Table 17, this nitrogen may marginally improve the coulombic efficiency compared to the electrolysis in air.

Table 16. Effect of the electrolysis current in a lower temperature (750 °C) lithium carbonate electrolyte on the electrolytic formation iron with coiled iron cathodes. Electrolyte is 3.0 m in Fe^{3+} and Li_2O.

Temperature (^oC)	750	750	750	750	750
Gas above electrolyte	**N₂**	**N₂**	**N₂**	**N₂**	**N₂**
Anode: Ni wire, d = 2.0 mm, l = 16 cm, coil, area:	$10\ cm^2$	$10\ cm^2$	$10\ cm^2$	$10\ cm^2$	$10\ cm^2$

Cathode: Fe coil, l = 26.5 cm, d =1.2 mm, area:	10 cm^2	10 cm^2	10 cm^2	10 cm^2	10 cm^2
Electrolysis current (A) during a 2 hour electrolysis	**0.25**	**0.5**	**1.0**	**2.0**	**4.0**
Coulombic efficiency (100% x Fe^0 mass exp/theory)	53.7	93.1	86.7	50.3	25.6

Table 17. Effect of the electrolysis temperature in a lithium carbonate electrolyte on the electrolytic formation iron with coiled <u>horizontal</u> nickel anodes and coiled wire iron cathodes. 1A, 2 hour electrolyses. Electrolyte is 3.0 m in Fe^{3+} and Li_2O.

Temperature (^{o}C)	**730**	**750**	**750**	**800**	**850**
Gas above electrolyte	**N_2**	**N_2**	air	air	air
Anode: Ni wire, d = 2.0 mm, l = 16 cm, coil, area:	10 cm^2	10 cm^2	10 cm^2	10 cm^2	10 cm^2
Cathode: Fe coil, l = 26.5 cm, d =1.2 mm, area:	10 cm^2	10 cm^2	10 cm^2	10 cm^2	10 cm^2
Coulombic efficiency (100% x Fe^0 mass exp/theory)	89.9	86.7	84.7	58.0	34.5
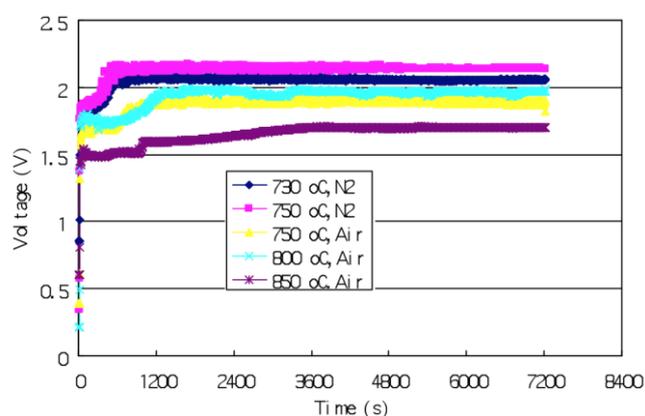
Figure 13. Variation of STEP Iron electrolysis potential at 1.0 A with electrolysis temperature lithium carbonate electrolyte. Electrolyses are conducted either under air or under nitrogen, as indicated on the figure.

Table 18 includes even higher coulombic efficiency STEP iron configurations. The first column contains the same anode on the surface separated by 1 cm from a cathode near the bottom of the cell. As seen in the second column, the use of a smaller (half) diameter nickel or iron wire for the anode and cathode decreases, rather than increases, the coulombic efficiency. We had been working under the hypothesis that hot oxygen would be deleterious to the metallic iron product. Hence, we had previously configured the anode above the cathode to allow gas to evolve without contacting the iron. Interestingly, in Table 18, at the lower temperature of 730°C in molten lithium carbonate, an opposite, inverted electrode configurations is not only functional, but can exhibit both improved coulombic efficiency and lower electrolysis potential. The coulombic efficiency of these inverted cells is at least 94 to 95% (and this may be considered a lower limit if any iron metal drops into the electrolyte during the cathode removal).

Photos of a vertical cathode inside the anode configuration are presented in Fig. 14. The potential during electrolysis of these inverted electrode configurations is presented in Figure 15. The random oscillations during the cathode on top configuration may be related to a temporary partial blockage of the cathode as anode gas evolved below, passes through this upper electrode. Electrolyte is 3.0 m in Fe^{3+} and Li_2O.

Table 18. Effect of the cathode location in molten 730°C lithium carbonate on the electrolytic formation iron. Electrolyte is 3.0 m in Fe^{3+} and Li_2O.

Temperature (^{o}C)	**730**	**730**	**730**	**730**
Gas above electrolyte	**N_2**	**N_2**	**N_2**	**air**
Time of electrolysis (h) at 1.0 amp	*2h*	*2h*	*1h*	*1h*
Cathode, tight coiled steel wire: Area (cm^2)	10 cm^2	10 cm^2	10 cm^2	10 cm^2
Size: Length $\times$ or diameter (cm)	26.5x0.12	**53x0.06**	26.5x0.12	26.5x0.12
Coil shape: horizontal (plate) or vertical (cylinder)	plate	plate	plate	vertical
Cathode above, below, or inside the anode	below	below	**above**	**inside**
Anode: Ni coiled wire: Area (cm^2)	10 cm^2	10 cm^2	10 cm^2	10 cm^2
Size: wire length $\times$ diameter (cm), prior to coiling	16x0.20	32x0.10	16x0.20	16x0.20
Coil shape: horizontal (plate) or vertical (cylinder)	plate	plate	plate	cylinder
Anode above, below, or outside the cathode	above	above	below	outside
Average Potential of electrolysis (V)	1.87	1.80	1.62	1.95
Coulombic efficiency (100% x Fe^0 mass exp/theory)	89.9	71.8	94.4	94.8

12

Figure 14. Vertical cylindrical configured electrodes used in the molten 730°C lithium carbonate electrolysis in which the cathode was placed inside the anode. Left, middle and right-hand photos respectively show the electrodes prior to the electrolysis, after electrolysis and after removal from the electrolyte, and finally after separation of the cathode from the anode.

The ongoing series of STEP Iron electrode electrolyses are each at 730°C, for 2 hours, but are conducted at 0.5, rather than 1.0 A, to probe a path to lower electrolysis potentials, while preserving, or further increasing, the high coulombic efficiencies of iron production. Photographs of these electrodes with various surface areas of the inner, vertical cathode and outer anode coiled electrodes are shown in Figure 17. As seen compared to Figure 15, in Fig. 16, the lower current substantially decreases the electrolysis potential, and as seen in Table 19, retains over 90% the coulombic efficiency. For the same 0.5 A current, a substantially larger surface area electrodes (20 cm^2 cathodes and 40 cm^2 anodes, providing lower current density conditions), lowers the electrolysis potential to less than 1.4 V as seen in Fig. 16, but also decreases the coulombic efficiency in the last column of Table 19.
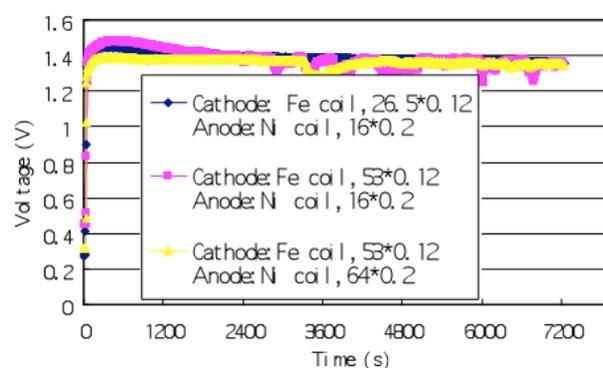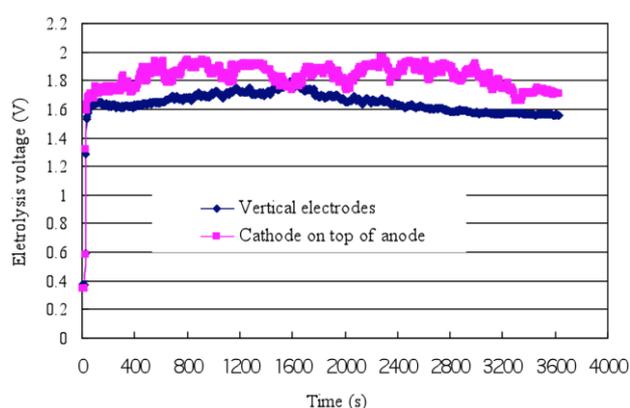
Figure 15 (left). Variation of STEP Iron electrolysis potential in a 730°C lithium carbonate electrolyte using the alternate vertical or inverted anode/cathode configurations.

Figure 16 (right). Variation of STEP Iron electrolysis potential in a 730°C lithium carbonate electrolyte using the vertical, inner coiled, cathode configuration with different electrode surface areas.

Figure 17. Vertical cylindrical configured, coiled electrodes with surface area varied by changing the length and coil diameter of the Ni (outer anode) or steel (inner cathode) wire as used in the molten 730°C lithium carbonate electrolysis.

Table 19. For the vertical anode situated outside the cathode configuration, the effect of current and electrode area on the iron formation in molten 730°C Li_2CO_3 containing 3.0 m Fe^{3+} and Li_2O.

Temperature (^{o}C)	**730**	**730**	**730**
Gas above electrolyte	**air**	**N$_2$**	**N$_2$**
Current & time of electrolysis	1.0A, *1h*	**0.5A, *2h***	0.5A, *2h*
Cathode, tight coiled steel wire: Area (cm^2)	10 cm^2	10 cm^2	**20 cm^2**
Size: Length $\times$ or diameter (cm) Coil shape: vertical (cylinder), inside the anode	26.5x0.12	26.5x0.12	**53.5x0.12**
Anode: Ni coiled wire: Area (cm^2)	10 cm^2	10 cm^2	**40 cm^2**
Size: wire length $\times$ diameter (cm), prior to coiling Coil shape: vertical (cylinder), outside the cathode	16x0.20	16x0.20	64x0.20
Coulombic efficiency (100%x Fe^0 mass exp/theory)	94.8	91.2	72.8

In an attempt to further prevent any parasitic reaction of the anode and cathode products, the next configuration, places an alumina tube between the outer (anode) and inner vertical, coiled electrodes. This configuration is photographed in Figure 18, and although the average electrolysis potential is high at 1.98 V, as seen in the second column of Table 20, the efficiency does improve. A return to the horizontal, coiled anode (above the cathode and with an alumina separator) retains very high coulombic efficiencies but creates high electrolysis potential. Compared to an average of 1.4 V electrolysis in the Figure 17

series of experiments, the next two electrolyses occur at an average, higher electrolysis potentials of 1.81V and 1.78 V respectively. In each case a 10 cm^2 cathode has a horizontal configuration and is located below the coiled, horizontal anode. The first utilizes the coiled steel wire and the second a coiled shim (4.8 x 0.65 cm foil) steel cathode. Reflecting the high columbic efficiencies summarized in the last two columns of Table 18, the high iron content of the product is evident, in Figure 19 both at the (uncoiled) shim cathode and still coiled wire cathode. An alternative, horizontal reticulated) Ni anode (consisting of a square 6.25 cm^2 area, 0.33 cm thick Ni sponge) above a vertical cathode supported electrolysis at an intermediate potential of 1.51 V. An expanded study of this latter anode, with high surface area morphology, will be presented at a future date.

Figure 18 (left). Configuration: outer Ni anode is alumina tube shielded & inside is the coiled steel wire cathode.

Figure 19. Photo of the high iron content at the (uncoiled) shim and still coiled wire cathodes after removal from the electrolytes summarized in

the last two columns of Table 19 in the molten 730°C lithium carbonate, electrolytic production of iron.

Table 20. The vertical anode inside anode configuration: effect of area and planar versus wire cathodes on the electrolytic formation of iron in molten 730°C Li$_2$CO$_3$ with 3.0 m Fe^{3+} and Li$_2$O.

Temperature (°C)	**730**	**730**	**730**	**730**
Gas above electrolyte	N$_2$	N$_2$	N$_2$	N$_2$
Current & time of electrolysis (	0.5A, *2h*	0.5A, *2h*	0.5A, *2h*	0.5A, *2h*
Cathode, tight coiled steel wire: Area (cm^2) Wire or shim (foil)	10 cm^2	**7.5 cm^2**	**6.25 cm^2**	**10 cm^2**
Size: Length × wire diameter or shim height (cm) Coil shape: horizontal (plate) or vertical (cylinder)	wire	wire in tube (Fig. 18)	**shim**	**wire**
	26.5x0.12	**20x0.12**	4.8x0.65	26.5x0.12
Wire Cathode above, below, or inside the anode	vertical	horizontal	vertical	vertical coil id x h: 1.3x0.65
	inside	**below**	below	below
Anode: Ni coiled wire: Area (cm^2)	10 cm^2	**5.7 cm^2**	**10 cm^2**	**10 cm^2**
Size: Length × diameter (cm) Coil shape: horizontal (plate) or vertical (cylinder)	16x0.20	9x0.20	32x0.10	32x0.10
Anode above, below, or outside the cathode	cylinder	coil	horizontal	horizontal
	outside	outside	above	above
Coulombic effic. (100%x Fe^0 mass exp/theory)	91.2	96.3	98.0	98.6

Further increases in coulombic efficiency and decrease in the energy needed to drive the STEP Iron are achieved with relatively small changes to the cathode. As seen in Table 21, replacement of the vertical inner coiled wire cathode with a similar shaped, steel shim (foil) cathode increases the coulombic efficiency. Furthermore, an increase in anode surface area (40 cm^2, compared to the 10 cm^2 in the first column of Table 20), decreases the electrolysis potential to 1.4 V. Further increases in the cathode diameter of these shim electrodes, with or without a "bottom" on the cathode (as pictured in Figure 20), decrease the electrolysis potential to less than 1.4 V (Figure 21), but, perhaps as a result of the increasing proximity of the anode, results in a decrease in the coulombic efficiency (Table 21). The time variation of the electrolysis potential for the high columbic efficiency is presented in Figure 21 and compared to similar configurations for the production of iron at 730°C in lithium carbonate containing 1.5 m in Fe$_2$O$_3$ and Li$_2$O.

Table 21. The vertical anode inside anode configuration: effect of electrode shape and area on the electrolytic formation iron at 730°C in molten Li$_2$CO$_3$ containing 3.0 m Fe^{3+} and Li$_2$O.

Temperature (°C)	**730**	**730**	**730**	**730**	**730**
Gas above electrolyte	N$_2$	N$_2$	N$_2$	N$_2$	N$_2$
Current & time of electrolysis	0.5A, *2h*	0.5A, *2h*	0.5A, *2h*	0.5A, *2h*	0.5A, *2h*
cathode (inside), vertical cylinder, area (cm^2) coiled steel wire or shim (foil)	10 cm^2	**3 cm^2**	**6 cm^2**	**9 cm^2**	**3 cm^2**
Length × wire diameter or shim height (cm)	wire	**shim**	**shim**	**shim**	**shim**
open or with solid bottom	26.5x0.12	**1.67x1.80**	**3.34x1.80**	**5x1.80**	**1.67x1.80**
	open	open	bottom	bottom	bottom
anode: Ni vertical wire coil or Ni crucible	10cm^2 coil	40cm^2 coil	40cm^2 coil	40cm^2 coil	**crucible**

Ni wire prior to coiling: length x diam (cm) coil or crucible diameter:	16x0.20	64x0.20	64x0.20	64x0.20	
	4.0 cm	4.0 cm	4.0 cm	4.0 cm	3.2 cm
Coulomb. effic. (100%x Fe^0 mass exp/theory)	91.2	100.0	97.5	47.6	98.2

Figure 20. Vertical steel shim electrodes placed inside the anode for STEP Iron electrolysis as described in Table 21.

The electrolysis configuration is simplified when the electrolysis is conducted in a nickel crucible which comprises both the anode and the cell body in one piece, and can further decrease the electrolysis potential. This configurations of the STEP Iron cell is presented in Figure 22; included is a photograph of the cathode after the electrolysis, with the product attached and including some solidified electrolyte). The iron electrolysis product is easy to remove and readily detaches from the cathode. As shown in Figure 21, the electrolysis potential is 1.35 V.
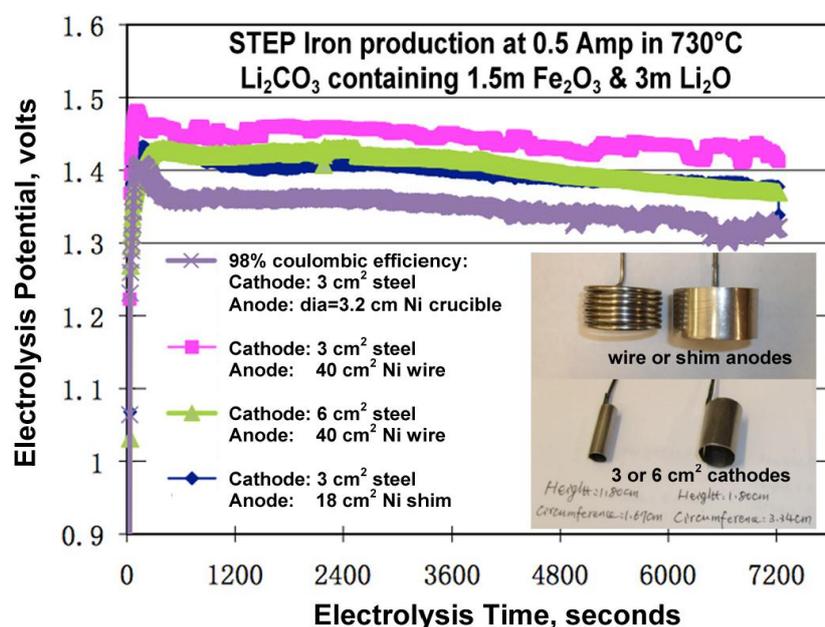
Figure 21. The variation of the electrolysis potential for the electrolytic production of iron. Inset: photographs of anodes (top) or cathodes (bottom) used in these electrolyses. During the electrolysis the cathode, immersed in the molten electrolyte, is situated within the anode.
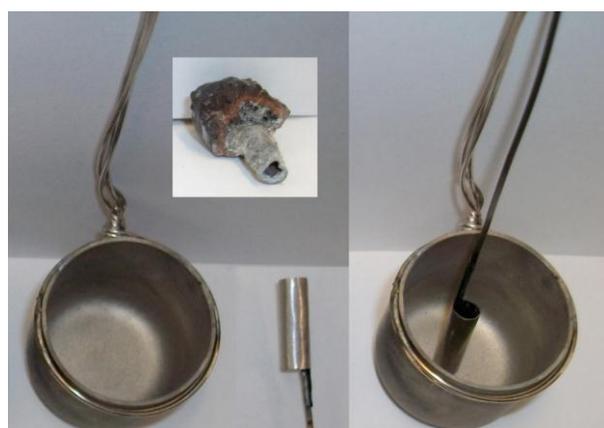
Figure 22. A nickel crucible serving as both cell wall and anode electrode. A vertical steel cylinder cathode is placed inside the crucible for STEP Iron electrolysis as described in the final column of Table 21. Inset photo: Cathode with product (and including some solidified electrolyte) after the electrolysis.

This electronic supplementary information provides a detailed characterization of the necessary electrolyte composition, temperature and electrochemical component proximity, size and shape for STEP Iron to provide high coulombic efficiency, at low electrolysis potential, while maintaining kinetically facile electron transfer. The coulombic efficiency approaches 100% yield of the 3 e- reduction of Fe_2O_3, The electrolysis potential is less than 1.4 V at a high (current density) rate of iron production. The iron electrolysis product contains iron and electrolyte, and is easy to remove, readily detaching from the cathode. A larger surface area cathode will lower this potential, but may lead to closer proximity to the anode which can decrease the iron coulombic efficiency. Opportunities to significantly decrease the electrolysis potential, while maintaining high cathode current densities, will likely be attained by moving from the largely planar oxygen electrode (anode) to

15

chemically, or mechanically roughened, high microscopic surface area electrodes, and/or using geometric shapes which will expose more of anode surface than the planar electrode.

Alternative carbonate electrolytes. A more cost effective solution to the corrosivity of the sodium-potassium STEP carbonate melt (than the use of iridium which is stable as an air electrode during 5 hours of electrolysis in 750°C $Na_{0.23}K_{0.77}CO_3$, compared to nickel air electrodes which corrode) is found by the addition of calcium carbonate or barium salts to the sodium-potassium, lithium-free, carbonate melt (the addition of calcium carbonate is shown here for the electrolytic formation of a carbon product from carbon dioxide splitting, rather than an iron product from iron oxide splittng).[12] The addition of calcium carbonate can decrease the melting point of a carbonate mix. The sodium/lithium carbonate mix, $Li_{1.07}Na_{0.93}CO_3$, has a melting point of 499°C, but decreases to below 450°C if 2 to 10 mol% equimolar $CaCO_3$ and $BaCO_3$ is added.

In addition to the sodium-potassium carbonate electrolytes, electrolyses are also conducted here in calcium-sodium-potassium electrolytes ranging up to a calcium fraction of $Ca_{0.27}Na_{0.70}K_{0.75}$. Electrodes used are presented in Figure 1. A nickel oxygen anode appears to be fully stable during extended (five hour) 0.5 A electrolyses at 750°C in this melt, using the 30 cm² nickel foil anode and a 7.0 cm² steel wire cathode, and the electrolysis proceeds at between 1.9 to 2.2V. Unlike the electrolyses conducted in the calcium free (sodium-potassium) carbonate melt, carbon forms and remains on the cathode during electrolysis, and the steel cathode remains the same diameter, as measured subsequent to the electrolysis. As shown subsequent to the electrolyses, in the cathode photographs at the bottom of Figure 1, electrolyses conducted in either $Ca_{0.16}Na_{1.03}K_{0.65}CO_3$ or $Ca_{0.27}Na_{0.70}K_{0.75}CO_3$ electrolytes exhibit a thick carbon product on the cathode, while this is not the case following electrolysis without calcium carbonate in $Na_{1.23}K_{0.77}CO_3$. The electrolysis potential and subsequent cathode product, during a repeat of the $Ca_{0.27}Na_{0.70}K_{0.75}CO_3$ electrolysis, but at a constant electrolysis current of 1A, rather than 0.5A, and utilizing a 21cm² (55 cm coiled steel wire) cathode is presented in Figure 2.
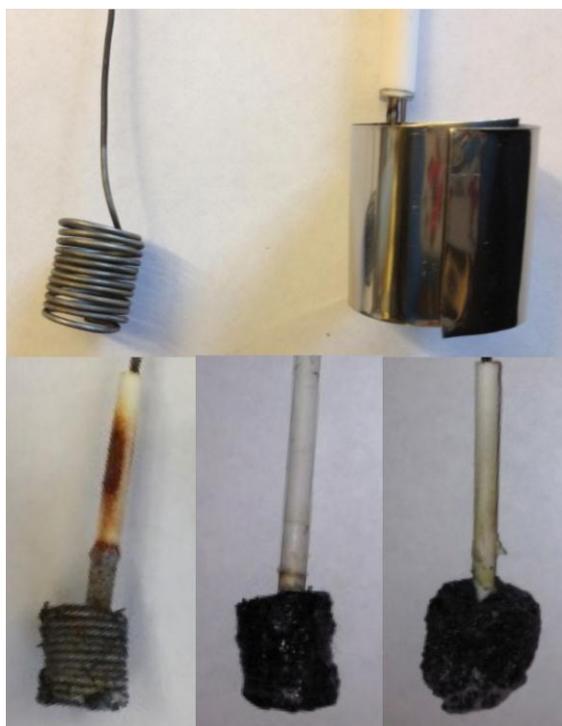
Figure 1. Top: Cathode (top left) and anode (top right) prior to 0.5 A, 5 hour lithium-free electrolyses at 750°C with increasing calcium carbonate concentration. The cathode is placed inside the anode, which are both immersed in the molten electrolyte. Bottom: Cathodes after electrolysis in lithium-free molten carbonates. Electrolytes used were respectively: $Na_{1.23}K_{0.77}CO_3$ (lower left cathode), $Ca_{0.16}Na_{1.03}K_{0.65}$ (lower middle cathode), and $Ca_{0.27}Na_{0.70}K_{0.75}$ (lower right cathode).
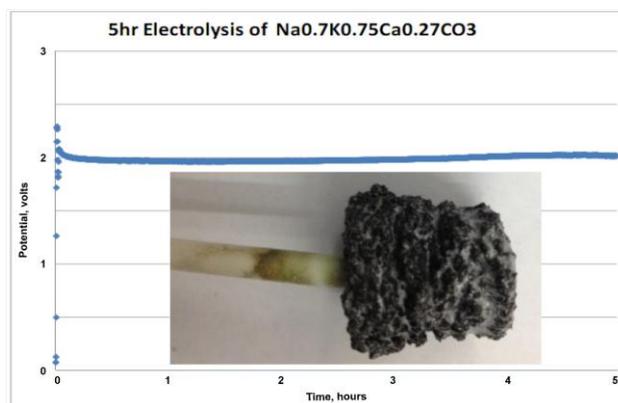
Figure 2. Time variation of the electrolysis potential during a five hour electrolysis at 1A in $Ca_{0.27}Na_{0.70}K_{0.75}CO_3$ at 750°C. Inset: cathode subsequent to the electrolysis.

References

ESI-1 A. J. deBethune, T. S. Licht, *J. Electrochem. Soc.*, 1959, **106**, 616.

ESI-2 J. O'M. Bockris, *Energy Options* (**1980**, Halsted Press, NY).

ESI-3 S. Licht, *J. Phys. Chem. B*, 2003, **107**, 4253.

ESI-4 S. Licht, L. Halperin, M. Kalina, M. Zidman, N. Halperin, *Chem. Comm.*, 2003, **2003**, 3006.